

PGCN: Progressive Graph Convolutional Networks for Spatial-Temporal Traffic Forecasting

Yuyol Shin

Civil and Environmental
Engineering

Korea Advanced Institute of
Science and Technology
Daejeon, South Korea
yuyol.shin@kaist.ac.kr

Yoonjin Yoon[†]

Civil and Environmental
Engineering

Korea Advanced Institute of
Science and Technology
Daejeon, South Korea
yoonjin@kaist.ac.kr

ABSTRACT

The complex spatial-temporal correlations in transportation networks make the traffic forecasting problem challenging. Since transportation system inherently possesses graph structures, much research efforts have been put with graph neural networks. Recently, constructing adaptive graphs to the data has shown promising results over the models relying on a single static graph structure. However, the graph adaptations are applied during the training phases, and do not reflect the data used during the testing phases. Such shortcomings can be problematic especially in traffic forecasting since the traffic data often suffers from the unexpected changes and irregularities in the time series. In this study, we propose a novel traffic forecasting framework called Progressive Graph Convolutional Network (PGCN). PGCN constructs a set of graphs by progressively adapting to input data during the training and the testing phases. Specifically, we implemented the model to construct progressive adjacency matrices by learning trend similarities among graph nodes. Then, the model is combined with the dilated causal convolution and gated activation unit to extract temporal features. With residual and skip connections, PGCN performs the traffic prediction. When applied to four real-world traffic datasets of diverse geometric nature, the proposed model achieves state-of-the-art performance with consistency in all datasets. We conclude that the ability of PGCN to progressively adapt to input data enables the model to generalize in different study sites with robustness.

CCS CONCEPTS

• Information systems → Data mining; • Applied computing → Transportation.

KEYWORDS

*Article Title Footnote needs to be captured as Title Note

[†]Corresponding Author

Permission to make digital or hard copies of part or all of this work for personal or classroom use is granted without fee provided that copies are not made or distributed for profit or commercial advantage and that copies bear this notice and the full citation on the first page. Copyrights for third-party components of this work must be honored. For all other uses, contact the owner/author(s).

KDD '22, August 14-18, 2022, Washington, D.C. USA

© 2022 Copyright held by the owner/author(s). 978-1-4503-0000-0/18/06...\$15.00

Spatial-temporal traffic forecasting, graph neural network, adaptive graph convolution, transportation, multivariate time-series

ACM Reference format:

Yuyol Shin and Yoonjin Yoon. 2022. Progressive Graph Convolutional Networks for Spatial-Temporal Traffic Forecasting. In *Proceedings of the 28th ACM SIGKDD Conference on Knowledge Discovery and Data Mining (KDD '22)*. ACM, New York, NY, USA, 9 pages.

1 Introduction

The traffic forecasting problem has long been studied as a crucial technical capability of intelligent transportation systems. The problem aims to predict future traffic states of transportation networks using historical observations. An accurate forecast of traffic states can be utilized in real-world applications such as travel time estimation [1] and prospective traffic navigation [2]. Yet, the complex spatial-temporal correlations in traffic data make the problem especially challenging.

Traditional approaches include statistical models such as ARIMA (Auto-Regressive Integrated Moving Average) [3] and VAR (Vector Auto-Regressive) [4], and machine learning models such as K-Nearest Neighbor [5] and Support Vector Regression [6]. Although these models showed advantages in interpretability of the model parameters, such models had limitations in capturing complex spatial-temporal correlation in traffic data, especially in the spatial domain.

In recent years, deep learning models have shown the ability to increase the scope and accuracy of traffic forecasting. Recurrent Neural Networks (RNN) have naturally gained popularity for their ability to process sequential data [7-10]. However, the gradient vanishing problem inherent in RNNs made them difficult to capture long-term relationships and the sequential computation of the models required prolonged training time. To overcome such limitations, convolutions have been introduced to extract temporal features [11-14]. Excluding the sequential computation, convolutions were able to learn temporal correlations without the gradient vanishing problem with less training time. The recently developed self-attention mechanism is also used in traffic forecasting problems [15-16].

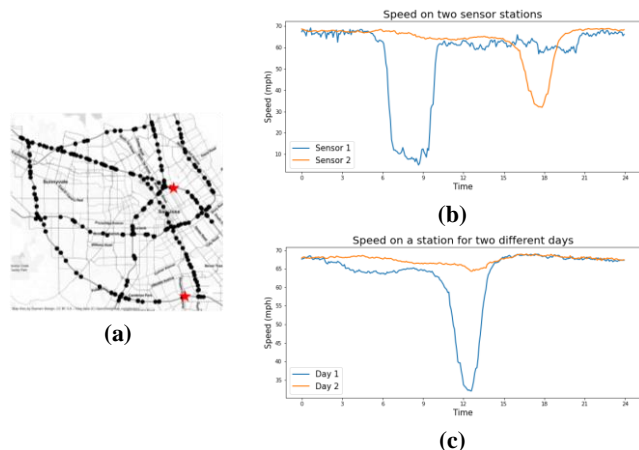


Figure 1. Example of time-varying spatial correlation.

For spatial feature extraction, earlier works mainly implemented Convolutional Neural Networks (CNN) [10, 17-18]. However, CNN could only operate in 2D space and is unable to reflect the topological structure of transportation networks. For such reason, Graph Neural Networks (GNN) have become a common choice to extract spatial features from the multiple nodes in a transportation network [8-10, 12-16]. The current state-of-the-art models for spatial-temporal traffic forecasting not only aggregate information from physically adjacent nodes, but also constructs adaptive graph based on data-driven methods. STF-GNN [19] constructs a dynamic graph using Dynamic Time Warping (DTW) distances [20] using train data. Graph WaveNet [13] makes the model to learn node embeddings during the training phase, and constructs the self-adaptive graph. DMSTGCN [14] tries to capture time-varying spatial correlations by constructing dynamic graphs for each time slot of a day. However, all these models define the graph during the training phases, and do not progressively adapt to the data used for forecasting. However, correlations between nodes can change by time even for the same time-of-days. In Figure 1(b), real-world traffic speed data from two sensors are plotted. Although two sensors are not adjacent in the transportation network, they share similar trends during off-peak hours. Moreover, it is shown in Figure 1(c) that speed trends on a sensor could change even for the same time-of-day. To aggregate information from appropriate nodes, a dynamic graph needs to capture the correlation that varies over the time.

In this work, we present a novel spatial-temporal traffic forecasting model, Progressive Graph Convolutional Networks (PGCN). The graph convolution module in the model first constructs a progressive graph that can adapt to the input data at both training and testing phases. Then, to reflect structural transportation network and overall randomness, a graph convolution is operated on the progressive graph, transition matrix, and self-adaptive graph [13]. In this way, the graph convolution module can capture spatial correlation among the nodes that are similar in geographical locations, and/or short/long-term trends. We implemented dilated causal convolution [21] to capture

temporal correlation. Convolution-based temporal feature extraction methods have advantages in computation time compared to RNNs, and less memory consumption compared to self-attention methods. The main contributions of our paper are as follows:

- We propose a novel spatial-temporal traffic forecasting model, Progressive Graph Convolution Network (PGCN). By constructing a progressive graph that can adapt to data, the model can capture the time-varying spatial correlation. Combined with dilated causal convolution, the model is designed to model complex spatial-temporal correlations in traffic data.
- A progressive graph constructor is implemented to model time-varying spatial correlation. Using cosine similarity and adjutor matrix, the graph can flexibly adapt to changing data even during the testing phase.
- Experiments on two real-world datasets demonstrate that the proposed model achieves state-of-the-art performance. Also, the model outperforms the baseline models even when the information on the structural network is not provided.

2 Related Works

2.1 Graph Neural Networks

Graph Neural Networks have been applied in a variety of research areas including protein structure prediction, citation network [29], recommender system [23], and action recognition [24] to learn graph-structured data. Also, in spatial-temporal forecasting, the GNNs have been a popular choice to extract spatial features. The networks under the umbrella of graph neural networks can be categorized into three groups – the convolutional, attentional, and message-passing GNNs [25] – having differences in how they aggregate information from neighboring nodes. The convolutional GNNs [8, 26-27] multiply a constant value to the source node features and conduct aggregating operations. The group of spectral graph convolutions constructs filter in Fourier domain and extracts spatial features [26-27]. There also is a group of spatial-based graph convolutions which defines the convolution based on the spatial relations among the nodes. GraphSAGE [28] samples a fixed number of neighbor nodes for each node and aggregates the information. Diffusion Convolution [8] defines the probability transition matrix for the nodes and regards the information propagation in the graphs as a diffusion process. The attentional GNNs calculate the multiplier with a function of the source node and target node features. Graph Attention Networks [29] implements the multi-head attention mechanism by using the concatenation of source and target nodes features as queries, learnable parameters as keys, and source node feature as values. GaAN [30] implements the attention method with an additional gate to control the information of neighbor nodes. The last category, message-passing computes the vector-based features as a function of the source and target nodes features [31-32].

2.2 GNNs for Spatial-Temporal Traffic Forecasting

While the most common form of graph neural networks takes the adjacency matrices with only structural connectivity information, there have been several efforts to incorporate more structural information in traffic forecasting. Li et al. [8] suggested to crop edges based on the geospatial distance among the nodes, reflecting the distance information of the transportation networks. DDP-GCN [33] showed incorporating various structural information such as distance, heading direction and joint angle could enhance the forecasting power of the models, and the MW-TGC network [10] showed that different structural characteristics should be considered in different scenarios. However, these methods all rely on static information such as distance between node pairs, the speed limit of road segments, and the joint angle of two nodes, while in spatial-temporal forecasting, nodes may share similar characteristics without being physically close, or connected. To reflect relativeness without physical connection, there has been an effort to construct semantic graphs based on functional similarity, and transportation connectivity [34]. There also have been efforts to construct graphs based on input data using Dynamic Time Warping distance [19]. Several works [13-14, 35] showed learning an adaptive graph during the training phase could enhance the performance of the model even further. Graph WaveNet [13] constructed an adaptive adjacency matrix by multiplying self-learned node embeddings, and DMSTGCN showed constructing one adaptive graph for each time slot of a day could enhance the performance even further. However, as far as the authors recognize, all these methods define the graphs before the validation and test phases. Since the trend of spatial-temporal data may confront changes in daily trends and other unexpected situations during testing time, there needs a method to adapt to the input data in both training and testing phases.

2.3 Temporal Feature Extraction

While GNNs have become a popular choice of spatial feature extraction, temporal feature extraction methods for spatial-temporal traffic forecasting have another group of choices. In the initial deep models for traffic forecasting, RNNs have been a popular choice as they naturally possess the ability to learn sequential data [7-10]. Another line of work implements temporal convolution [12, 31, 36], which is much lighter in terms of computation expense. However, the models had to be deeper to increase the size of the reception field and to overcome such limitation, dilated convolutions are implemented [13-14]. As self-attention made a large advancement in the field of natural language processing recently, a few models implements the attention mechanism [15-16]. There are also studies where temporal features are extracted by constructing a graph incorporating temporal connectivity and conducting graph convolution operation on the graph [19, 37].

3 Preliminaries

3.1 Notations and Definitions

Definition 3.1 (Transportation Network Graph). We represent the transportation network as a directed graph $\mathcal{G} = (V, E)$, where V is a set of N nodes and E is a set of edges representing pairwise connection between the nodes. An adjacency matrix $\mathbf{A} = (A_{ij}) \in \mathbb{R}^{N \times N}$ is a square Boolean matrix where the nodes $v_i, v_j \in V$ are connected by an edge $(v_i, v_j) \in E$.

Definition 3.2 (Graph Signal). The signal from node v_i at time t is denoted as $\mathbf{x}_t^i \in \mathbb{R}^C$ where C is the number of input features. The graph signal is denoted as $\mathbf{X}_t = [\mathbf{x}_t^1, \mathbf{x}_t^2, \dots, \mathbf{x}_t^N] \in \mathbb{R}^{N \times C}$. The signals of node v_i observed during the last T time steps from time t are denoted $\mathbf{x}_t^{i(T)} \in \mathbb{R}^{T \times C}$. Similarly, $\mathbf{X}_t^{(T)} \in \mathbb{R}^{T \times N \times C}$ is the graph signal for the entire graph.

3.2 Problem Definition

The traffic forecasting problem is to predict future traffic states using historical traffic states such as speed, flow, and occupancy. Given the historical data of T time steps from time t , the problem is defined as:

$$H: [\mathbf{X}_{t-T+1}, \mathbf{X}_{t-T+2}, \dots, \mathbf{X}_t, \mathcal{G}] \rightarrow [\hat{\mathbf{Y}}_{t+1}, \hat{\mathbf{Y}}_{t+2}, \dots, \hat{\mathbf{Y}}_{t+T'}], \quad (1)$$

where $\hat{\mathbf{Y}}_{t+k}$ is the predicted traffic state at time $t+k$, ($1 \leq k \leq T'$), and T' is the number of time steps to predict. In this study, we consider traffic data of single feature, which yields $C = 1$.

4 Progressive Graph Convolutional Networks

In this section, we explain the core idea of Progressive Graph Convolutional Networks (PGCN). We first explain the procedure for constructing a progressive graph, and graph convolution operation using progressive adjacency matrix. Then, we describe the implementation of dilated causal convolution combined with the graph convolution module. Lastly, the overall framework of PGCN is illustrated.

4.1 Progressive Graph Construction

The similarity between two node signals changes over time. For example, while the morning peak hours of near schools and office buildings are similar, the afternoon peak hours can be quite different. Modeling such correlations based on static features such as POI category or speed limit is intuitive, but it might not be the most efficient approach considering the scale and complexity involved. Instead, we propose to learn rich semantics hidden in the online traffic data itself by measuring node similarities beyond the simple spatial adjacency.

In this study, we propose the progressive graph that can progressively adapt to the traffic change based on node signal similarities. Wu et al. [13] and Han et al. [14] employed similar ideas to adaptively learn the adjacency matrices. However, their methods update the graph during the training phase only and did not incorporate the online changes during the testing phase.

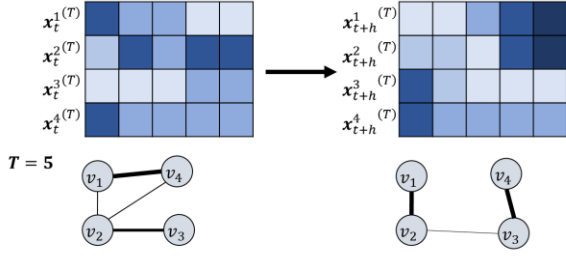


Figure 2. Progressive graph. Each row in the matrix is the illustration of node signal profile given the last 5 time steps. At t , v_1 shows the highest similarity with v_4 , but such connection disappears at $t + h$.

Definition 4.1. Progressive Graph (p-graph). As the correlations between different nodes evolve over time, it is intuitive to update the node relationship progressively using online data. Progressive graph (p-graph) $\{\mathcal{G}^t\}$ is a set of graphs, where $\mathcal{G}^t = (V, A_p^t)$. Here, A_p^t is the progressive adjacency matrix at time t , which contains the pairwise weights learned from the node signal similarities.

The goal is to impose a higher weight between nodes with similar signals regardless of their spatial proximity. The node similarities are measured using the cosine similarity of their signals. The cosine similarity s_{ij} between two nodes v_i and v_j is defined as:

$$s_{ij}^t = \tilde{\mathbf{x}}_t^{i(T)\top} \cdot \tilde{\mathbf{x}}_t^{j(T)}, \quad (2)$$

where $\tilde{\mathbf{x}}_t^{i(T)} = \bar{\mathbf{x}}_t^{i(T)} / \|\bar{\mathbf{x}}_t^{i(T)}\|$ is a unit vector, and $\bar{\mathbf{x}}_t^{i(T)}$ is the min-max normalized signal of node v_i at time t . To make the similarity learn randomness, we implemented a learnable adjustor matrix $\mathbf{W}_{adj} \in \mathbb{R}^{T \times T}$, and each element of the progressive adjacency matrix $A_{p_{ij}}^t$ is

$$A_{p_{ij}}^t = \text{softmax} \left(\text{ReLU} \left(\tilde{\mathbf{x}}_t^{i(T)\top} \mathbf{W}_{adj} \tilde{\mathbf{x}}_t^{j(T)} \right) \right). \quad (3)$$

The softmax function is applied to normalize the progressive adjacency matrix, and ReLU activation eliminates the negative connections.

Figure 2 illustrates the idea of the progressive graph. Given four nodes $\{v_1, v_2, v_3, v_4\}$, each row in the matrix illustrates the node signal observed in the last $T = 5$ time steps. We present two matrices for time t and $t + h$. At t , one can observe strong similarity between v_1 and v_4 , whereas v_1 is most similar to v_2 at time $t + h$. It is also notable that edges can appear/disappear over time.

4.2 Progressive Graph Convolution Module

The core idea of any graph convolution module is to aggregate neighbor nodes' information in extracting spatial features for the target node. The basic form of graph convolution module is multiplying graph signal and learnable parameter to adjacency matrix processed by a defined method. In traffic forecasting, one of the most popular forms of graph convolution module is

Diffusion Convolution [8], in which traffic flow on a transportation network is considered as a diffusion process. With the transition matrix $\mathbf{P} = \mathbf{A} / \text{rowsum}(\mathbf{A})$, the diffusion convolution on a directed graph for K -step diffusion process with filter f_W can be defined as

$$\mathbf{Z}_t = \mathbf{X}_t \star_{\mathcal{G}} f_W = \sum_{k=0}^{K-1} \mathbf{P}^k \mathbf{X}_t \mathbf{W}_{k,1} + \mathbf{P}^{\top k} \mathbf{X}_t \mathbf{W}_{k,2}, \quad (4)$$

where $\star_{\mathcal{G}}(f_W)$ is the graph convolution operation with filter f_W , and $\mathbf{W}_{k,1}$, and $\mathbf{W}_{k,2} \in \mathbb{R}^{C \times D}$ are learnable parameters. \mathbf{P} and \mathbf{P}^{\top} are used to reflect the forward and backward diffusion process. If given adjacency matrix is undirected, only the first term of equation (4) is used.

Taking the diffusion convolution as the base graph convolution module for our progressive graph convolution, we added the multiplication of the progressive adjacency matrix, a graph signal matrix, and an additional weight parameter to diffusion convolution.

$$\mathbf{Z}_t = \mathbf{X}_t \star_{\mathcal{G}} f_W = \sum_{k=0}^{K-1} \left(\mathbf{P}^k \mathbf{X}_t \mathbf{W}_{k,1} + \mathbf{P}^{\top k} \mathbf{X}_t \mathbf{W}_{k,2} + \mathbf{A}_p^t \mathbf{X}_t \mathbf{W}_{k,3} \right) \quad (5)$$

4.3 Dilated Causal Convolution

In PGCN, we implement dilated causal convolution [21] to extract temporal features of graph signals. Causal convolutions extract temporal features by stacking 1-D convolution layers while ensuring that future information is not considered for prediction. This operation can be conducted as in Figure 3(a), shifting the output features of each convolution layer by a few time steps. Since the main component of the causal convolution is convolution layers, it does not require sequential computation as in recurrent units. Compared to the self-attention layer, which has become another popular choice in time-series modeling, causal convolutions require a smaller number of learnable parameters, thus making a model more concise. Dilated causal convolution is to overcome the limitation of causal convolution that it has to use many layers to increase the size of the reception field. By skipping inputs values by defined dilation factor, the size of the reception field can increase exponentially with the number of hidden layers (Figure 3(b)). Given a single feature time-series input $\mathbf{x}_t^{i(T)} \in \mathbb{R}^T$ at time t , and a convolution kernel $\boldsymbol{\gamma} \in \mathbb{R}^P$, the dilated causal convolution applied on $\mathbf{x}_t^{i(T)}$ can be represented as:

$$\mathbf{x}_t^{i(T)} \star_{\mathcal{T}} \boldsymbol{\gamma} = \sum_{p=0}^P \boldsymbol{\gamma}(p) \mathbf{x}_t^{i(T)}(t - d \times p), \quad (6)$$

where $\star_{\mathcal{T}}(\boldsymbol{\gamma})$ is dilated convolution operation with kernel $\boldsymbol{\gamma}$ d is the dilation factor, and scalar values in the parenthesis indicate the indices of the vectors. Finally, the temporal feature of the input sequence $\mathbf{X}_t^{(T)} \in \mathbb{R}^{N \times T \times C}$ is extracted by passing the input to gated activation units following the dilated causal convolution:

$$\mathbf{H}_t = \tanh(\boldsymbol{\Gamma}_1 \star_{\mathcal{T}} \mathbf{X}_t^{(T)}) \odot \sigma(\boldsymbol{\Gamma}_2 \star_{\mathcal{T}} \mathbf{X}_t^{(T)}), \quad (7)$$

where $\boldsymbol{\Gamma}_1$ and $\boldsymbol{\Gamma}_2 \in \mathbb{R}^{P \times C \times D}$ are the kernels for dilated casual convolutions, \odot denotes the element-wise multiplication, and $\sigma(\cdot)$ is a sigmoid activation function.

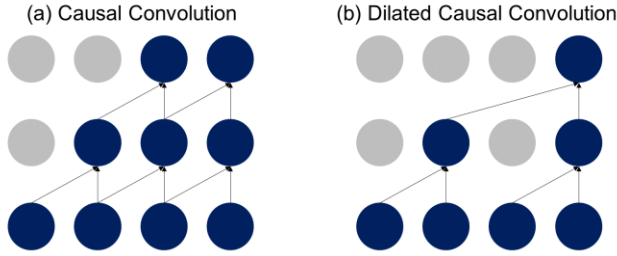


Figure 3. Causal Convolution and Dilated Causal Convolution

4.4 Overall Architecture of PGCN

Figure 4 shows the overall architecture of PGCN. Each spatial-temporal layer consists of dilated casual convolutions, a gated activation unit, a progressive graph convolution module, and a residual connection. While multiple spatial-temporal layers are stacked to increase the size of the reception field in temporal feature extraction, the parameter for progressive graph constructor is shared across the layers. Finally, the output layer consists of a skip connection from each layer to prevent information loss from the initial layers and two fully connected layers with ReLU activation. We used mean absolute error (MAE) for training.

$$MAE(\hat{Y}_t^{(T)}, Y_t^{(T)}) = \frac{1}{TN} \sum_{i=1}^N \sum_{j=0}^{T-1} |\hat{y}_{t-j}^i - y_{t-j}^i| \quad (8)$$

5 Experiments

5.1 Datasets

To evaluate the performance of the proposed model, we applied the model to four real-world datasets¹, namely, PeMS-Bay, METR-LA [8], Urban-core [38], and Seattle-Loop [9].

PeMS-Bay is a highway speed dataset for traffic forecasting collected by California Transportation Agencies (CalTrans) Performance Measurement System (PeMS). The dataset includes 6 months of data aggregated in the frequency of 5 minutes. Spatially, it consists of 325 loop detectors in the Bay area are included.

METR-LA is a highway traffic flow dataset containing the data collected from 207 loop detectors in Los Angeles County. The dataset contains 3 months of data aggregated in the frequency of 5 minutes. For PeMS-Bay and METR-LA, we used the same data preprocessing procedures as in Li et al. [8].

Urban-core is an urban speed dataset containing data collected from DTG (Digital Tacho Graph) on Seoul Taxis. The dataset includes speed data aggregated at road segment level in 5-minute resolution for the duration of 1 month. The number of road segments in the dataset is 304.

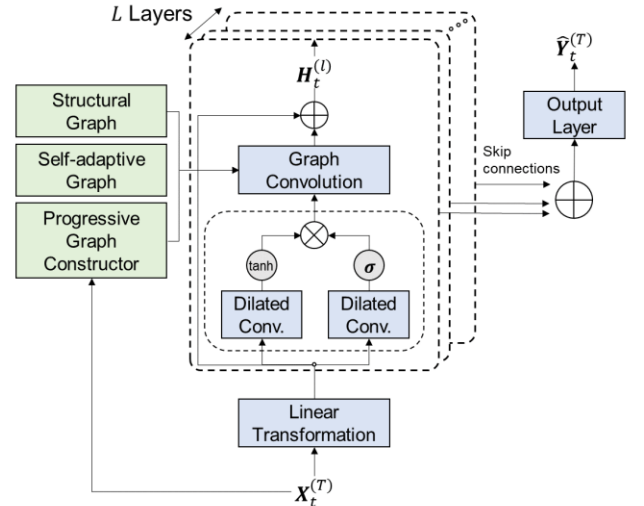


Figure 4. The overall architecture of PGCN

Table 1. Summary of the datasets

Datasets	# Samples	# Nodes	Frequency	Traffic
PeMS-Bay	52,116	325	5 min	Speed
METR-LA	34,272	207	5 min	Flow
Urban-core	8,640	304	5 min	Speed
Seattle-Loop	105,120	323	5 min	Speed

Seattle-Loop is a highway speed dataset collected from 323 loop detectors in the Greater Seattle Area. The dataset contains 5-minute resolution data for the entirety of 2015.

The training, validation, and test sets are divided in a proportion of 0.7, 0.1, and 0.2 for PeMS-Bay, METR-LA, and Seattle-Loop. For Urban-core, we used 21 days, 2 days, and 7 days division. Table 1 contains the summary of the datasets.

5.2 Experiment Settings

For metrics, we chose Mean Absolute Error (MAE), Root Mean Squared Error (RMSE), and Mean Absolute Percentage Error (MAPE). MAE is as defined in equation (8), and RMSE and MAPE can be defined as:

$$RMSE(\hat{Y}_t^{(T)}, Y_t^{(T)}) = \sqrt{\frac{1}{TN} \sum_{i=1}^N \sum_{j=0}^{T-1} (\hat{y}_{t-j}^i - y_{t-j}^i)^2} \quad (9)$$

$$MAPE(\hat{Y}_t^{(T)}, Y_t^{(T)}) = \frac{1}{TN} \sum_{i=1}^N \sum_{j=0}^{T-1} \frac{|\hat{y}_{t-j}^i - y_{t-j}^i|}{y_{t-j}^i}. \quad (10)$$

¹ Code and dataset are available at <https://github.com/yuyolshin/PGCN>

Table 2. Forecasting outcomes of PGCN and baseline models on four real-world datasets

	Model	15 min			30 min			60 min		
		MAE	RMSE	MAPE	MAE	RMSE	MAPE	MAE	RMSE	MAPE
PeMS-Bay	HA	1.60	3.43	3.24	2.18	4.99	4.65	3.05	7.01	6.83
	FC-LSTM	2.05	4.19	4.80	2.20	4.55	5.20	2.37	4.96	5.70
	DCRNN	1.38	2.95	2.90	1.74	3.97	3.90	2.07	4.74	4.90
	Graph WaveNet	1.30	2.74	2.73	1.63	3.70	3.67	1.95	4.52	4.63
	TGC-GRU	2.34	4.30	5.08	2.44	4.64	5.40	2.57	5.01	5.78
	GMAN	1.34	2.82	2.81	1.62	3.72	3.63	1.86	4.32	4.31
	DMSTGCN	1.33	2.83	2.80	1.67	3.79	3.81	1.99	4.54	4.78
	PGCN	1.30	2.73	2.72	1.62	3.67	3.63	1.92	4.45	4.55
METR-LA	HA	4.02	8.69	9.39	5.09	11.13	12.21	6.80	14.21	16.71
	FC-LSTM	3.44	6.30	9.60	3.77	7.23	10.90	4.37	8.69	13.20
	DCRNN	2.77	5.38	7.30	3.15	6.45	8.80	3.60	7.60	10.50
	Graph WaveNet	2.69	5.15	6.90	3.07	6.22	8.37	3.53	7.37	10.01
	TGC-GRU	5.25	8.56	12.45	5.99	10.37	14.18	7.32	13.47	17.11
	GMAN	4.04	8.53	10.26	4.59	9.85	11.69	5.33	11.21	13.60
	DMSTGCN	2.85	5.54	7.54	3.26	6.56	9.19	3.72	7.55	10.96
	PGCN	2.70	5.16	6.98	3.08	6.22	8.38	3.54	7.36	9.94
Urban-core	HA	3.05	4.68	11.77	3.47	5.16	13.69	4.03	5.83	16.26
	FC-LSTM	2.73	4.02	11.20	2.74	4.03	11.24	2.80	4.10	11.51
	DCRNN	2.44	3.74	9.53	2.68	4.01	10.76	2.90	4.29	11.86
	Graph WaveNet	2.56	3.88	9.88	2.89	4.26	11.47	3.27	4.72	13.27
	TGC-GRU	2.76	4.05	11.3	2.79	4.09	11.44	2.82	4.13	11.63
	GMAN	2.70	4.02	11.01	2.75	4.08	11.23	2.86	4.20	11.79
	DMSTGCN	2.42	3.70	9.42	2.62	3.94	10.44	2.81	4.17	11.37
	PGCN	2.39	3.70	9.27	2.60	3.94	10.31	2.78	4.15	11.16
Seattle-Loop	HA	3.54	5.84	8.83	4.22	7.34	11.30	5.42	9.61	15.78
	FC-LSTM	3.72	6.02	10.95	3.92	6.46	11.70	4.25	7.12	13.11
	DCRNN	2.83	4.76	7.38	3.28	5.84	9.38	3.86	7.07	12.01
	Graph WaveNet	3.10	5.11	8.35	3.68	6.37	10.83	4.50	7.94	14.55
	TGC-GRU	3.78	6.08	10.86	4.03	6.67	11.86	4.38	7.44	13.46
	GMAN	2.97	4.86	8.15	3.34	5.71	9.97	3.79	6.61	11.57
	DMSTGCN	3.05	5.18	8.41	3.60	6.32	10.86	4.42	7.77	14.35
	PGCN	2.85	4.80	7.56	3.28	5.80	9.46	3.82	6.94	11.86

For the experiment of PGCN, we implemented the model with 8 spatial-temporal layers and set the number of hidden dimensions to 32. For dilated causal convolutions, dilation factors are 1, 2, 1, 2, 1, 2, 1, and 2 with a convolution kernel size of 2. We used Adam optimizer for the training with the initial learning rate of 0.001. We ran the model for 100 epochs and chose the model that best performed in the validation set for evaluation. The model was trained in Pytorch environment with one NVIDIA TITAN RTX with 24GB memory (GPU) and Intel(R) Xeon(R) CPU ES-2630 v4 @ 2.20GHz (CPU).

5.3 Methods for Comparison

To evaluate the performance of the proposed model, we compared the experimental results with the following baseline models:

- HA (Historical Average). In our experiments, only the traffic state of the most recent time step is used to predict the following steps.
- FC-LSTM combines LSTM units with a fully connected layer.
- DCRNN combines the diffusion convolution layer with recurrent units to make the spatial-temporal prediction.
- TGC-GRU uses Traffic Graph Convolution [9] with recurrent units. Free-flow matrices, and additional loss terms are omitted in experiments in this study.
- GMAN implements attention mechanisms to extract both spatial and temporal features. Then, pass the features through the transform attention layer to make predictions.
- DMSTGCN constructs adaptive graph for each time slot of a day and conducts graph convolution operation. In our

experiments, we did not implement the layer for auxiliary information modeling.

5.4 Experimental Results

5.4.1 Overall performance evaluation. Table 2 shows the performance of the proposed model and the baselines on the four datasets for 15, 30, and 60 minutes predictions. In all datasets, deep neural network models outperformed the historical average forecasting except for TGC-GRU in METR-LA, and TGC-GRU and FC-LSTM in Seattle-Loop on 15-min prediction. In the PeMS-Bay dataset, convolution and attention-based models have shown improved performance over RNN-based models (FC-LSTM, DCRNN, and TGC-GRU). In the METR-LA dataset, however, DCRNN showed higher forecasting power than one convolution model (DMSTGCN) and the attention model (GMAN). In the Urban-core dataset, all deep neural network models produced similar levels of prediction outcomes except for Graph WaveNet, and lastly, in Seattle-Loop, DCRNN, GMAN, and PGCN yielded competitive performances. PGCN achieves the best performance in at least one performance metric in all tasks except predictions for 60-min on PeMS-Bay, 15-min on METR-LA, 15-min, and 60-min for Seattle-Loop. Although it does not always significantly outperform the other models in all datasets, our model is shown to be the model with the most consistent results. This indicates that constructing graphs that can adapt to data during the testing phase is important in forecasting traffic states to achieve competitive performances with consistency in different application sites. In our opinion, the ability to adapt to real-time data helps the model obtain robustness against unexpected changes and irregularities in time-series compared to the other models with adaptive graphs (Graph WaveNet and DMSTGCN). Compared to GMAN, extracting spatial features from neighboring nodes using GCN could help avoid the overfitting problem for PGCN, since GMAN calculates attention scores between all possible node pairs. The average rank for all prediction horizons is in Table 3.

5.4.2 Evaluation of the Progressive Graph Convolution. We conducted an ablation study on the graph convolution module to verify the performance of the proposed model. We tested graph convolution operations with different combinations of adjacency matrices from 3 graph structures, which were transition (T) matrix,

Table 3. Average ranking of each model in different datasets.

	PeMS-Bay	METR-LA	Urban-core	Seattle-Loop	Overall
HA	6.9	7.0	8.0	7.1	7.3
FC-LSTM	6.6	5.1	4.1	5.9	5.4
DCRNN	5.0	3.1	4.0	1.9	3.5
GWNet	2.5	1.3	6.0	5.3	3.8
TGC-GRU	7.6	7.7	5.4	6.7	6.8
GMAN	2.2	6.2	4.9	2.1	3.9
DMSTGCN	3.8	3.9	2.2	5.0	3.7
PGCN	1.5	1.7	1.3	1.9	1.6

Table 4. Result of ablation study of progressive adjacency matrix on the PeMS-Bay and METR-LA.

	Graph Convolution	MAPE		
		15 min	30 min	60 min
PeMS-Bay	P	2.90	4.11	5.72
	P + SA	2.88	4.09	5.73
	T + SA	2.73	3.67	4.63
	T + P (PGCN)	2.72	3.63	4.55
	T + P + SA	2.73	3.74	4.73
METR-LA	P	7.84	10.03	13.24
	P + SA	7.43	8.90	10.33
	T + SA	6.90	8.37	10.01
	T + P (PGCN)	6.98	8.38	9.94
	T + P + SA	7.05	8.48	10.13
Urban-core	P	9.78	11.37	13.28
	P + SA	9.33	10.39	11.25
	T + SA	9.88	11.47	13.27
	T + P (PGCN)	9.27	10.31	11.16
	T + P + SA	9.27	10.36	11.18
Seattle-Loop	P	8.10	10.44	14.09
	P + SA	7.80	9.69	12.05
	T + SA	8.35	10.83	14.55
	T + P (PGCN)	7.56	9.46	11.86
	T + P + SA	7.56	9.20	11.13

self-adaptive (SA) adjacency matrix [13], and progressive (P) adjacency matrix.

Table 4 shows the MAPE of the different graph convolution modules on 15, 30, and 60-min predictions. In the PeMS-Bay and Urban-core datasets, the combination of the transition matrix and progressive adjacency matrix showed the best performances in all prediction horizons. In the METR-LA dataset, the combination of the transition matrix and self-adaptive adjacency matrix outperformed the transition-p-graph combination in 15-min and 30-min predictions. In the Seattle-Loop dataset, the combination of using all three types of adjacency matrices produces the best outcome in all prediction horizons. The results show again that no model can outperform the others in every

scenario. However, the combination of the transition matrix and progressive adjacency matrix produces the most consistent results against the changes in the environment. Also, it is notable that the model achieves competitive performances when two adaptive adjacency matrices are used together. When the graph structure is unavailable, the choice of the progressive and self-adaptive matrices could offer a sound alternative to traffic forecasting tasks.

In Figure 5, the speeds of two sensors in the PeMS-Bay dataset and 12 steps moving average of weights between them are illustrated for a day. Before the morning peak begins for sensor 401936 at 9 AM, two nodes share similar traffic trends. The weights between them are not very high at this time because most of the nodes share similar traffic trends (free-flow) before the morning peak begins. However, it is observed that when the peak

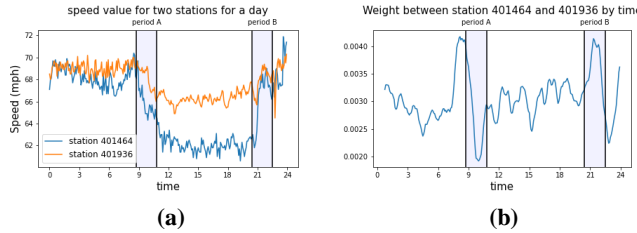


Figure 5. Traffic speed and weights for two stations in PeMS-Bay dataset.

begins, the differences in the rate of speed change results in the low learned similarity value. In addition, the two nodes share similar traffic trends during the afternoon although the actual speed values are different. Counting on the similarity of the traffic trend, the similarity values are even higher than the period before the morning peak. Finally, when the nodes coincidentally recover the free-flow speed, the similarity value increases by a large margin. This demonstrates the ability of the proposed model to progressively adapt to the data used for the task, and capture the spatial correlations between nodes in transportation networks.

5.4.3 Computation Efficiency. While progressively adapting to the online data, PGCN still captures computation efficiency compared to other spatial-temporal graph neural networks. Among the adaptive graph constructor, progressive adjacency matrix requires the least number of parameters. Self-adaptive adjacency matrix [13] is constructed by multiplying source and target node embedding matrices E_1 and $E_2 \in \mathbb{R}^{N \times d}$. Although DMSTGCN alleviates some of the computation burden, the number of parameters to construct the dynamic graph [14] is higher compared to the self-adaptive adjacency matrix and progressive graph. embedding of time slots $E^t \in \mathbb{R}^{N_t \times d}$, embedding of source and target nodes E_1 and $E_2 \in \mathbb{R}^{N \times d}$, and a core tensor $E^k \in \mathbb{R}^{d \times d \times d}$, where N_t is the number of time slots in a day (288 for the datasets used in this study). The progressive adjacency matrix only requires an adjutor matrix $W_{adj} \in \mathbb{R}^{T \times T}$, where T is the length of the historical traffic states. Yet, PGCN generalize better than Graph WaveNet and DMSTGCN to more study sites.

Table 5 describes the computation time and the number of total parameters for PGCN, DCRNN, Graph WaveNet, DMSTGCN and GMAN on the PeMS-Bay dataset.

Table 5. The number of parameters and computation cost on the PeMS-Bay Dataset

Model	# Params	Computation Time	
		Training (s/epoch)	Inference
PGCN	305,404	104.2	4.0
DCRNN	223,744	177.1	13.4
Graph WaveNet	311,760	103.6	4.6
DMSTGCN	351,692	59.1	2.0
GMAN	513,795	845.7	25.5

6 Conclusions

In this paper, we proposed a spatial-temporal traffic forecasting model, Progressive Graph Convolutional Networks (PGCN). The proposed model captures the time-varying spatial correlations by progressively adapting to data used for forecasting tasks. Instead of fixing adaptive graphs after the training phase, we used adjusted cosine similarity of traffic speeds to make the graph flexible even during the testing phase. The experimental results show that the model with a progressive graph can consistently achieve state-of-the-art performance in all four of the datasets used in this study. The model showed the ability to generalize in multiple datasets, proving the necessity of reflecting online input data to acquire robustness. In future work, we will work on implementing the progressive graph convolution to extract both spatial and temporal features.

ACKNOWLEDGMENTS

This work was supported by the National Research Foundation of Korea (NRF) Basic Research Lab grant (2020R1A2C2010200) and Midcareer Research Grant (2021R1A4A1033486) by South Korean government.

REFERENCES

- [1] Fang, X., Huang, J., Wang, F., Zeng, L., Liang, H., & Wang, H. (2020, August). Constgat: Contextual spatial-temporal graph attention network for travel time estimation at baidu maps. In Proceedings of the 26th ACM SIGKDD International Conference on Knowledge Discovery & Data Mining (pp. 2697-2705).
- [2] Jing Yuan, Yu Zheng, Chengyang Zhang, Wenlei Xie, Xing Xie, Guangzhong Sun, and Yan Huang. T-drive: driving directions based on taxi trajectories. In GIS, pages 99–108, 2010.
- [3] Williams, B. M., Hoel, L. A.: Modelling and forecasting vehicular traffic flow as a seasonal ARIMA process. Journal of Transportation Engineering 129(6), 664-672 (2003).
- [4] Chandra, S. R., Al-Deek, H: Predictions of freeway traffic speeds and volumes using vector autoregressive models. Journal of Intelligent Transportation System 13(2), 53-72 (2009).
- [5] Zhang, L., Liu, Q., Yang, W., Wei, N., & Dong, D. (2013). An improved k-nearest neighbor model for short-term traffic flow prediction. Procedia-Social and Behavioral Sciences, 96, 653-662.
- [6] Wu, C. H., Ho, J. M., & Lee, D. T. (2004). Travel-time prediction with support vector regression. IEEE transactions on intelligent transportation systems, 5(4), 276-281.
- [7] X. Ma, Z. Tao, Y. Wang, H. Yu, and Y. Wang, "Long short-term memory neural network for traffic speed prediction using remote microwave sensor data," Transp. Res. C, Emerg. Technol., vol. 54, pp. 187–197, May
- [8] Y. Li, R. Yu, C. Shahabi, and T. Liu, "Diffusion convolutional recurrent neural network: Data-driven traffic forecasting," in Proc. Int. Conf. Learn. Represent., Vancouver, BC, Canada, May 2018, pp. 1–16.
- [9] Cui, Z., Henrickson, K., Ke, R., & Wang, Y. (2019). Traffic graph convolutional recurrent neural network: A deep learning framework for network-scale traffic learning and forecasting. IEEE Transactions on Intelligent Transportation Systems, 21(11), 4883-4894.
- [10] Shin, Y., & Yoon, Y. (2020). Incorporating dynamicity of transportation network with multi-weight traffic graph convolutional network for traffic forecasting. IEEE Transactions on Intelligent Transportation Systems.
- [11] S. Guo, Y. Lin, S. Li, Z. Chen, and H. Wan, "Deep spatial-temporal 3D convolutional neural networks for traffic data forecasting," IEEE Trans. Intell. Transp. Syst., vol. 20, no. 10, pp. 3913–3926, Oct. 2019
- [12] Yu, B., Yin, H., & Zhu, Z. (2017). Spatio-temporal graph convolutional networks: A deep learning framework for traffic forecasting. arXiv preprint arXiv:1709.04875.
- [13] Wu, Z., Pan, S., Long, G., Jiang, J., & Zhang, C. (2019, January). Graph WaveNet for Deep Spatial-Temporal Graph Modeling. In IJCAI.
- [14] Han, L., Du, B., Sun, L., Fu, Y., Lv, Y., & Xiong, H. (2021, August). Dynamic and Multi-faceted Spatio-temporal Deep Learning for Traffic Speed Forecasting. In Proceedings of the 27th ACM SIGKDD Conference on Knowledge Discovery & Data Mining (pp. 547-555).

- [15] Cai, L., Janowicz, K., Mai, G., Yan, B., & Zhu, R. (2020). Traffic transformer: Capturing the continuity and periodicity of time series for traffic forecasting. *Transactions in GIS*, 24(3), 736-755.
- [16] Zheng, C., Fan, X., Wang, C., & Qi, J. (2020, April). Gman: A graph multi-attention network for traffic prediction. In *Proceedings of the AAAI Conference on Artificial Intelligence* (Vol. 34, No. 01, pp. 1234-1241).
- [17] Y. Wu, H. Tan, L. Qin, B. Ran, and Z. Jiang, "A hybrid deep learning based traffic flow prediction method and its understanding," *Transp. Res. C, Emerg. Technol.*, vol. 90, pp. 166-180, May 2018
- [18] Ma, X., Dai, Z., He, Z., Ma, J., Wang, Y., & Wang, Y. (2017). Learning traffic as images: a deep convolutional neural network for large-scale transportation network speed prediction. *Sensors*, 17(4), 818.
- [19] Li, M., & Zhu, Z. (2021, May). Spatial-temporal fusion graph neural networks for traffic flow forecasting. In *Proceedings of the AAAI conference on artificial intelligence* (Vol. 35, No. 5, pp. 4189-4196).
- [20] Müller, M. (2007). Dynamic time warping. *Information retrieval for music and motion*, 69-84.
- [21] van den Oord, Aaron, Kalchbrenner, Nal, Vinyals, Oriol, Espeholt, Lasse, Graves, Alex, and Kavukcuoglu, Koray. Conditional image generation with PixelCNN decoders. *CoRR*, abs/1606.05328, 2016b. URL <http://arxiv.org/abs/1606.05328>.
- [22] Xia, T., & Ku, W. S. (2021, August). Geometric graph representation learning on protein structure prediction. In *Proceedings of the 27th ACM SIGKDD Conference on Knowledge Discovery & Data Mining* (pp. 1873-1883).
- [23] Wu, S., Tang, Y., Zhu, Y., Wang, L., Xie, X., & Tan, T. (2019, July). Session-based recommendation with graph neural networks. In *Proceedings of the AAAI conference on artificial intelligence* (Vol. 33, No. 01, pp. 346-353).
- [24] Shi, L., Zhang, Y., Cheng, J., & Lu, H. (2019). Skeleton-based action recognition with directed graph neural networks. In *Proceedings of the IEEE/CVF Conference on Computer Vision and Pattern Recognition* (pp. 7912-7921).
- [25] Bronstein, M. M., Bruna, J., Cohen, T., & Velicković, P. (2021). Geometric deep learning: Grids, groups, graphs, geodesics, and gauges. *arXiv preprint arXiv:2104.13478*.
- [26] Defferrard, M., Bresson, X., & Vandergheynst, P. (2016). Convolutional neural networks on graphs with fast localized spectral filtering. *Advances in neural information processing systems*, 29.
- [27] Kipf, T. N., & Welling, M. (2016). Semi-supervised classification with graph convolutional networks. *arXiv preprint arXiv:1609.02907*.
- [28] Hamilton, W., Ying, Z., & Leskovec, J. (2017). Inductive representation learning on large graphs. *Advances in neural information processing systems*, 30.
- [29] Veličković, P., Cucurull, G., Casanova, A., Romero, A., Lio, P., & Bengio, Y. (2017). Graph attention networks. *arXiv preprint arXiv:1710.10903*.
- [30] Zhang, J., Shi, X., Xie, J., Ma, H., King, I., & Yeung, D. Y. (2018). Gann: Gated attention networks for learning on large and spatiotemporal graphs. *arXiv preprint arXiv:1803.07294*.
- [31] Gilmer, J., Schoenholz, S. S., Riley, P. F., Vinyals, O., & Dahl, G. E. (2017, July). Neural message passing for quantum chemistry. In *International conference on machine learning* (pp. 1263-1272). PMLR.
- [32] Battaglia, P. W., Hamrick, J. B., Bapst, V., Sanchez-Gonzalez, A., Zambaldi, V., Malinowski, M., ... & Pascanu, R. (2018). Relational inductive biases, deep learning, and graph networks. *arXiv preprint arXiv:1806.01261*.
- [33] Lee, K., & Rhee, W. (2022). DDP-GCN: Multi-graph convolutional network for spatiotemporal traffic forecasting. *Transportation Research Part C: Emerging Technologies*, 134, 103466.
- [34] Geng, X., Li, Y., Wang, L., Zhang, L., Yang, Q., Ye, J., & Liu, Y. (2019, July). Spatiotemporal multi-graph convolution network for ride-hailing demand forecasting. In *Proceedings of the AAAI conference on artificial intelligence* (Vol. 33, No. 01, pp. 3656-3663).
- [35] Wu, Z., Pan, S., Long, G., Jiang, J., Chang, X., & Zhang, C. (2020, August). Connecting the dots: Multivariate time series forecasting with graph neural networks. In *Proceedings of the 26th ACM SIGKDD International Conference on Knowledge Discovery & Data Mining* (pp. 753-763).
- [36] Guo, S., Lin, Y., Li, S., Chen, Z., & Wan, H. (2019). Deep spatial-temporal 3D convolutional neural networks for traffic data forecasting. *IEEE Transactions on Intelligent Transportation Systems*, 20(10), 3913-3926.
- [37] Song, C., Lin, Y., Guo, S., & Wan, H. (2020, April). Spatial-temporal synchronous graph convolutional networks: A new framework for spatial-temporal network data forecasting. In *Proceedings of the AAAI Conference on Artificial Intelligence* (Vol. 34, No. 01, pp. 914-921).
- [38] Shin, Y., & Yoon, Y. (2021). A Comparative Study on Basic Elements of Deep Learning Models for Spatial-Temporal Traffic Forecasting. *arXiv preprint arXiv:2111.07513*.